

Effect of electrode configuration on recognizing uterine contraction with electrohysterogram: Analysis using a convolutional neural network

Hao, D., Song, X., Qiu, Q., Xin, X., Yang, L., Liu, X., Jiang, H. & Zheng, D.

Author post-print (accepted) deposited by Coventry University's Repository

Original citation & hyperlink:

Hao, D, Song, X, Qiu, Q, Xin, X, Yang, L, Liu, X, Jiang, H & Zheng, D 2021, 'Effect of electrode configuration on recognizing uterine contraction with electrohysterogram: Analysis using a convolutional neural network', *International Journal of Imaging Systems and Technology*, vol. 31, no. 2, pp. 972-980.
<https://dx.doi.org/10.1002/ima.22505>

DOI 10.1002/ima.22505

ISSN 0899-9457

ESSN 1098-1098

Publisher: Wiley

This is the peer reviewed version of the following article: Hao, D, Song, X, Qiu, Q, Xin, X, Yang, L, Liu, X, Jiang, H & Zheng, D 2021, 'Effect of electrode configuration on recognizing uterine contraction with electrohysterogram: Analysis using a convolutional neural network', *International Journal of Imaging Systems and Technology*, vol. 31, no. 2, pp. 972-980, which has been published in final form at <https://doi.org/10.1002/ima.22505>. This article may be used for non-commercial purposes in accordance with Wiley Terms and Conditions for Self-Archiving.

Copyright © and Moral Rights are retained by the author(s) and/ or other copyright owners. A copy can be downloaded for personal non-commercial research or study, without prior permission or charge. This item cannot be reproduced or quoted extensively from without first obtaining permission in writing from the copyright holder(s). The content must not be changed in any way or sold commercially in any format or medium without the formal permission of the copyright holders.

This document is the author's post-print version, incorporating any revisions agreed during the peer-review process. Some differences between the published version and this version may remain and you are advised to consult the published version if you wish to cite from it.

Effect of Electrode Configuration on Recognizing Uterine Contraction with Electrohysterogram: Analysis Using a Convolutional Neural Network

Dongmei Hao¹, Xiaoxiao Song¹, Qian Qiu¹, Xin Xin², Lin Yang¹, Xiaohong Liu³, Hongqing Jiang^{#4}, Dingchang Zheng^{*5}

1. Faculty of Environment and Life Sciences, Beijing University of Technology, Intelligent Physiological Measurement and Clinical Translation, Beijing International Platform for Scientific and Technological Cooperation, Beijing 100024, China

2. Obstetrics Department, Shandong Provincial Qianfoshan Hospital, Jinan, 250014, China

3. Beijing Yes Medical Devices Company Limited, Beijing 100052, China

4. Beijing Haidian Maternal and Children Health Hospital, Beijing 100080, China

5. Centre for Intelligent Healthcare, Faculty of Health and Life Science, Coventry University, Priory Street, Coventry, United Kingdom CV1 5FB

*1 Corresponding author, Dongmei Hao, E-mail: haodongmei@bjut.edu.cn; Dingchang Zheng, E-mail: dingchang.zheng@coventry.ac.uk

#4 Hongqing Jiang, Co-first author

Abstract

There is a significant indicator of the pregnant uterus is uterine contraction (UC) in clinic. Electrohysterogram (EHG), recorded by electrodes on the abdominal of the pregnant, has recently been used as a promising method for monitoring UC. This paper aimed to evaluate the effect of various electrode configurations on applying a convolutional neural network (CNN) to recognize UCs with EHG signals. In this study, the EHG signals were in the Icelandic 16-electrode EHG database. Seven 8-electrode configurations and thirteen 4-electrode configurations were selected from the 4×4 electrode grid in the database. EHG signals from these selected electrode configurations were divided into UC and non-UC sections of 45s and saved as images. A CNN was modeled with convolutional, max-pooling, and fully connected layers. Each 8-electrode configuration with 7152 images and each 4-electrode configuration with 3576 images were applied to train CNN to recognize UCs, respectively. In the light of the area under the curve (AUC) and the accuracy, a scoring method was proposed to evaluate the effect of different electrode configurations on recognizing the UCs. The EHG signals from the 4-electrode configuration which covered the upper left of the uterus showed the best classification performance (AUC=0.79, Accuracy=0.72, Score=2.30). To conclude, the study could be utilized to optimize the electrode configuration, reduce the number of electrodes, and improve the feasibility of a practical application.

KEYWORDS Electrohysterogram (EHG), electrode configuration, uterine contraction (UC), convolutional neural network (CNN)

1 INTRODUCTION

Uterine contraction (UC) is a phenomenon of the myometrium associated with pregnancy or labor.¹ An important feature of labor is regular UCs, which are accompanied by the disappearance and expansion of the cervix.² When the pregnant are in labor, they will feel the UCs gradually frequent and synchronous until the labor is completed.³ Recording of UCs is a routine procedure of obstetrical care during pregnancy and labor, which provides important information for obstetricians. The current clinical approaches to assess UCs are manual palpation, external tocodynamometry (TOCO) and intrauterine pressure catheter (IUPC). Palpation is low-priced and no risks but a trained clinical observer is always needed. External TOCO is non-invasive, but the location of the sensor, tension of the elastic strap, properties of the maternal abdominal wall (fat thickness, abdominal muscles), and size of the uterus determines its recording quality. TOCO is an indirect indication of UC, and its interpretation depends on the clinician's subjectivity. Internal IUPC is confined to the invasion and infection.⁴ Therefore, there is an urgent clinical need to develop alternatives to detect UC.

UCs are produced by electrical activity in the myometrium. Electrohysterogram (EHG) is representative of the electrical activity of the uterine muscle, and therefore can be measured for monitoring and analyzing uterine contractility, which contributes to a better understanding of labor.⁵⁻⁶ Compared with TOCO, EHG has a better ability of contraction detection.⁷⁻⁸ In general, multiple electrodes were placed on the abdominal surface of the pregnant to record EHG signals.

Among the published studies with different research objectives, the number and configuration of electrodes were various. Icelandic EHG database presents 122 EHG recordings with a 4×4 electrode grid, which enables an independent and novel analysis of multi-electrode EHG for labor forecasts and other uses in obstetrical nursing.⁹ The term-preterm EHG database (TPEHG DB) contains 300 EHG signals recorded by four electrodes placed 3.5cm to the left, right, above and below the navel in a square.¹⁰ Similarly, several studies for prediction preterm labor also recorded EHG signals by four electrodes (symmetric about the navel) with different positions and inter-electrode distance.¹¹⁻¹² In the early diagnosis of preterm labor, eight electrodes were symmetrically arranged in two columns around the navel.¹³ During labor, six bipolar electrodes were utilized to recognize UCs, with three of which were horizontally along the basal region and the others above pubic symphysis at a distance of 300, 200, and 100 mm, respectively.¹⁴ Five cross form unshielded Ag / AgCl electrodes were used under the umbilicus to achieve a high signal/noise ratio.¹⁵ A patch with four monopolar electrodes in a diamond shape¹⁶ and an 8×8 high-density electrode grid¹⁷ have been applied to estimate EHG signal conduction velocity. However, the poor sensitivity of spatial selectivity and propagation direction of UC propagation with the conventional disc electrode impaired the accuracy of the measurements. Concentric ring electrodes have been investigated to recognize the electrical activity and additional information for inferring the efficiency of the uterus.¹⁸⁻¹⁹ A Spanish team evaluated the bipolar, tripolar, and quadripolar laplacian estimates via concentric ring electrodes.²⁰

More electrodes can provide comprehensive and abundant information about uterine activities. On the other hand, it can cause inconvenience for clinical practice. Therefore, the effect of electrode configuration on recognizing UCs has to be investigated, which may contribute to optimize electrode configuration, reduce the number of electrodes and obtain the most useful information for UC recognition.

A large number of linear and nonlinear characteristics have been fetched from multi-electrode EHG signals to differentiate labor and pregnancy contractions.²¹⁻²² Various feature selection methods combined with multiple classifiers have been attempted to select the relevant features for UC classification and reduce computational complexity.²² The performance of conventional classifiers such as support vector machine,²³ and artificial neural network (ANN)^{12, 24} depend on their input features. The convolutional neural network (CNN) is a kind of deep and feed-forward ANNs²⁵, which can make strong and mostly right assumptions about the input data for classification.²⁶ CNN has incredible

advantages in automatically obtaining the optimal features from training data without adding feature extraction and selection algorithm compared with the conventional classifiers.²⁷ Its depth and breadth can control the learning capacity of CNN. CNN has been applied to detect ventricular ectopic beats by electrocardiograph (ECG) signals with high accuracy.²⁸ It is worth investigating its ability to detect UCs by using EHG signals.

The objective of the research was to establish a CNN to investigate the effect of different electrode configurations on UC recognition, and therefore optimize the electrode configuration to reduce the number of electrodes for recording EHG signals.

2 METHODS

2.1 Icelandic 16-electrode EHG database

The EHG signals in the Icelandic 16-electrode database were recorded by an array of 4×4 electrodes placed on the abdomen, as shown in Figure 1.⁹ Electrode 9 to 12 were placed on the median axis of the uterus, and electrode 10 and 11 on halfway between the uterine fundus and pubic symphysis. The distance between centers of adjacent electrodes was 17.5mm. The ground and reference electrodes were positioned on the patient's hip. The recordings of 45 participants were collected, 122 in all, lasting 0.5-1 hour. The gestational age was between 29 weeks +5 days to 41 weeks+5 days. Participants had normal singleton pregnancies. The records included 112 late pregnancies and 10 labors. Fifty-seven recordings used synthetic oxytocin during pregnancy and labor. In addition to the EHG recordings, the database contained TOCO recordings, event comments, and obstetric cases of participants.

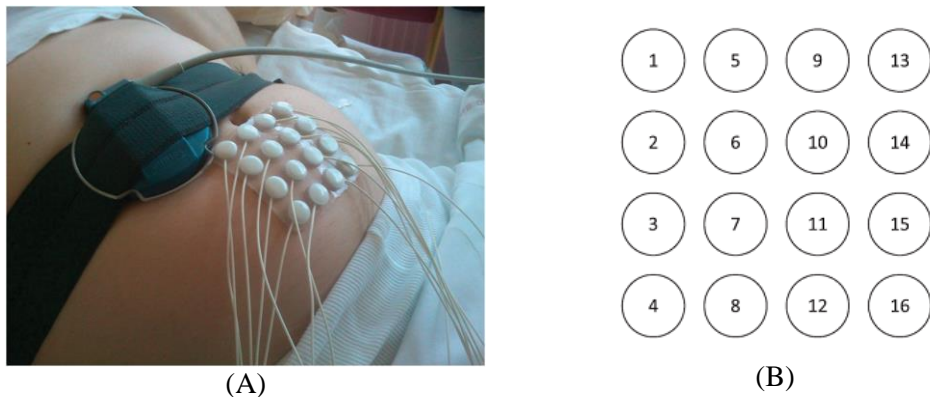


FIGURE 1 The Icelandic 16-electrode EHG recording placement.⁹ (A) The electrodes and TOCO on the abdomen of a pregnant woman (B) Numbering scheme of EHG electrode, as seen when looking at the abdomen of the pregnant

2.2 Selection of EHG electrode configuration

2.2.1 8-electrode and 4-electrode configuration

There are quantities of electrode combinations, among which eight and four electrodes have been used to predict preterm labor in previous studies.¹⁰⁻¹³ Concerning the 16-electrode configuration in the Icelandic EHG Database, there were $C(16,8)=12870$ types of 8-electrode configuration and $C(16,4)=1820$ types of 4-electrode configuration. Where C represented the number of combinations. Among them, seven 8-electrode configurations and thirteen 4-electrode configurations were selected based on the uterus shape, as shown in Figure 2. Among the 8-electrode configurations, 8H1-8H3 were along the horizontal direction, 8V1-8V3 were perpendicular, and 8I was in the form of an inverted cone-like uterus. Among the 4-electrode configurations, 4I-4IV were at the left and right, upper and bottom, and 4V at the center of the abdomen, 4V1-4V4 along the vertical direction, and 4H1-4H4 along the horizontal direction.

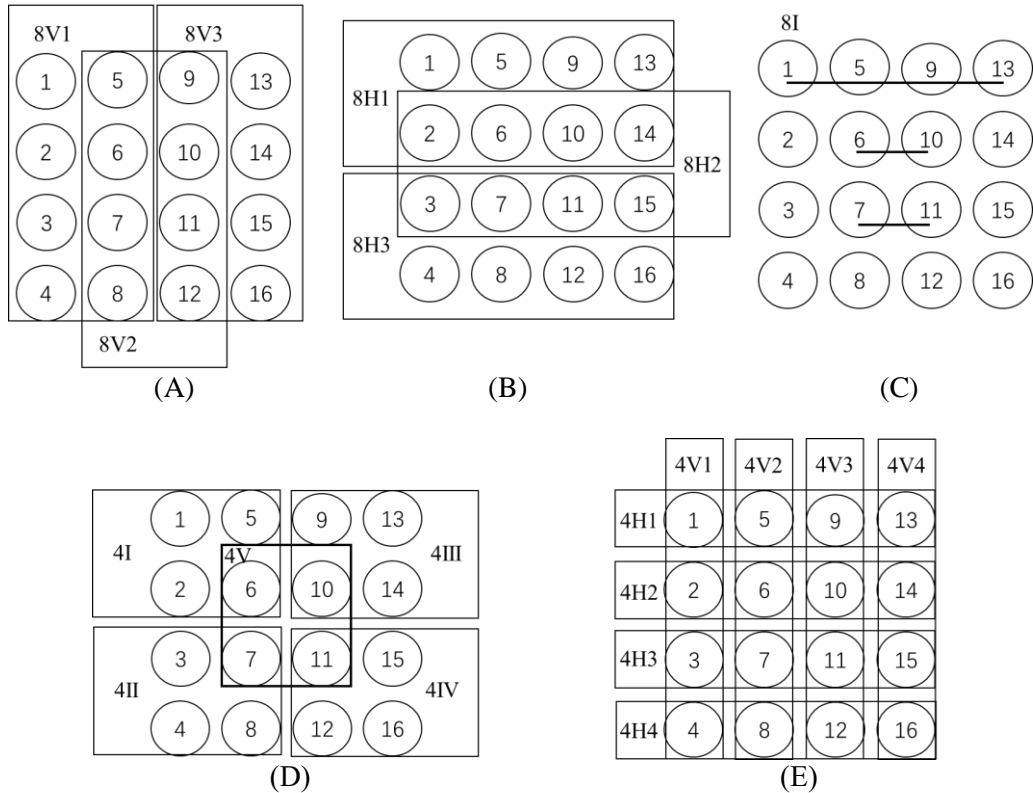
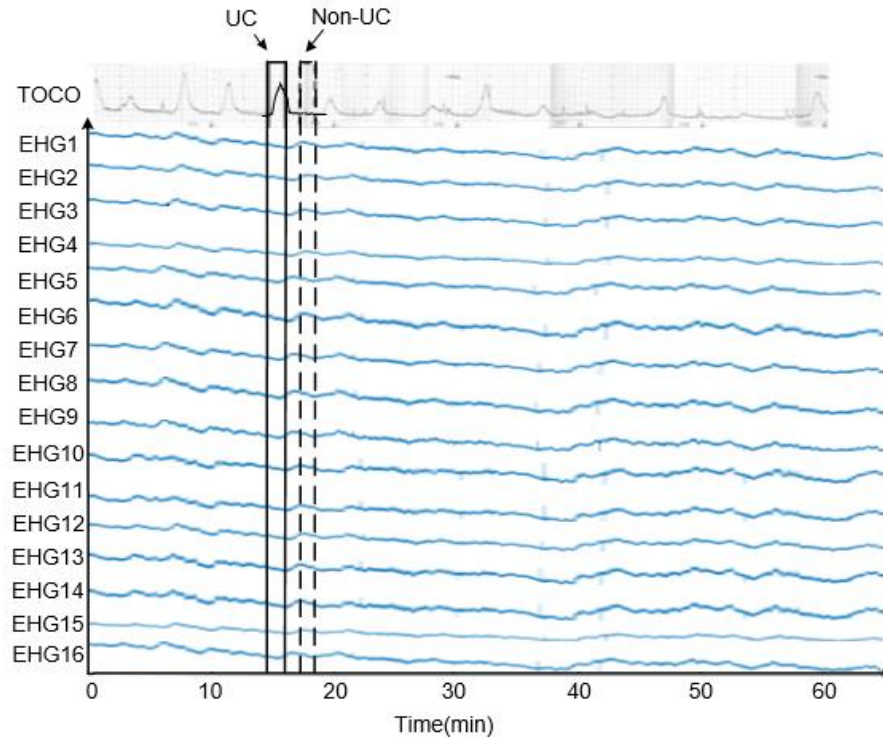


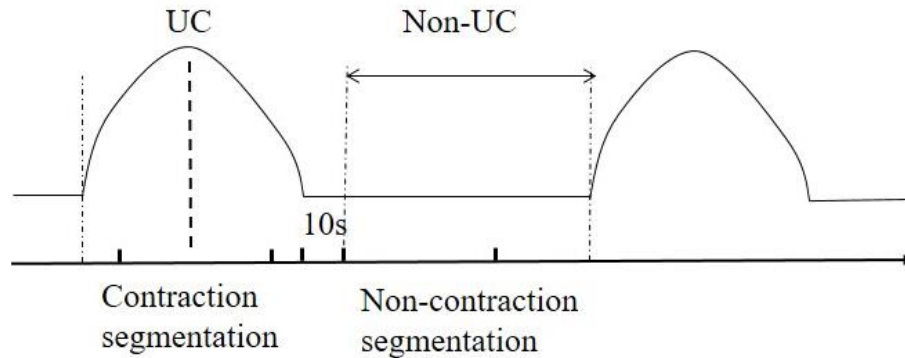
FIGURE 2 The selected electrode configurations. (A) 8V1-8V3 are along the vertical direction. (B) 8H1-8H3 along the horizontal direction. (C) 8I is in the form of an inverted cone. (D) 4I, 4II, 4III, 4IV, and 4V are at the four corners and center of the abdomen. (E) 4H1, 4H2, 4H3, and 4H4 are along the horizontal direction, and 4V1, 4V2, 4V3, and 4V4 are along the vertical direction.

2.2.2 EHG signal processing and segmentation

It has been reported that EHG signal is a low frequency signal of 0-5 Hz.²⁹ Firstly, the recorded EHG signals were filtered by 0.08 ~ 4Hz band-pass filter to clear baseline wander, power-line interference, maternal ECG and motion artifacts up. Next, there was a one-to-one relationship between the EHG segment and UC based on the TOCO and the UC comments. The duration of a UC is approximately 30~60s clinically. Therefore, the EHG segment of 45s corresponding to UC was obtained, and the corresponding non-UC EHG segment of 45s was obtained 10s after that UC. All EHG segments were then kept as 482 × 482 pixel images.



(A)



(B)

FIGURE 3 EHG and TOCO signals from the Icelandic 16-electrode EHG database. (A) An example of 16-channel EHG and TOCO signals (B) Time reference in the TOCO signal used to segment UC and non-UC EHG.

2.2.3 The architecture of the convolutional neural network

In this study, CNN was employed to classify the corresponding EHG segments of UCs and non-UCs. As shown in Figure 4, the CNN architecture was based on the exiting Alex-net structure,²⁶ which consisted of convolution (Conv), max-pooling, and fully connected (FC) layers. Conv layers utilized rectified linear unit (ReLU) and local response normalization (LRN), and FC layers utilized ReLU, dropout and softmax functions. Max-pooling layer was designed to downsample inputs without affecting the recognition capability. The ReLU with nonlinear activation function was employed to quick the forward propagation process and overcome the question of gradient explosion. Some neurons were randomly ignored in the training process by the dropout layer to alleviate the over-fitting problem. The kernel size and stride were determined from the trade-off between the effective features and the

number of feature maps. The kernel size and stride were usually larger in the first Conv layer to reduce the image size and computational complexity for the following layers. Preliminary tests optimized all the parameters. Table 1 summarizes the detailed parameters of the CNN established.

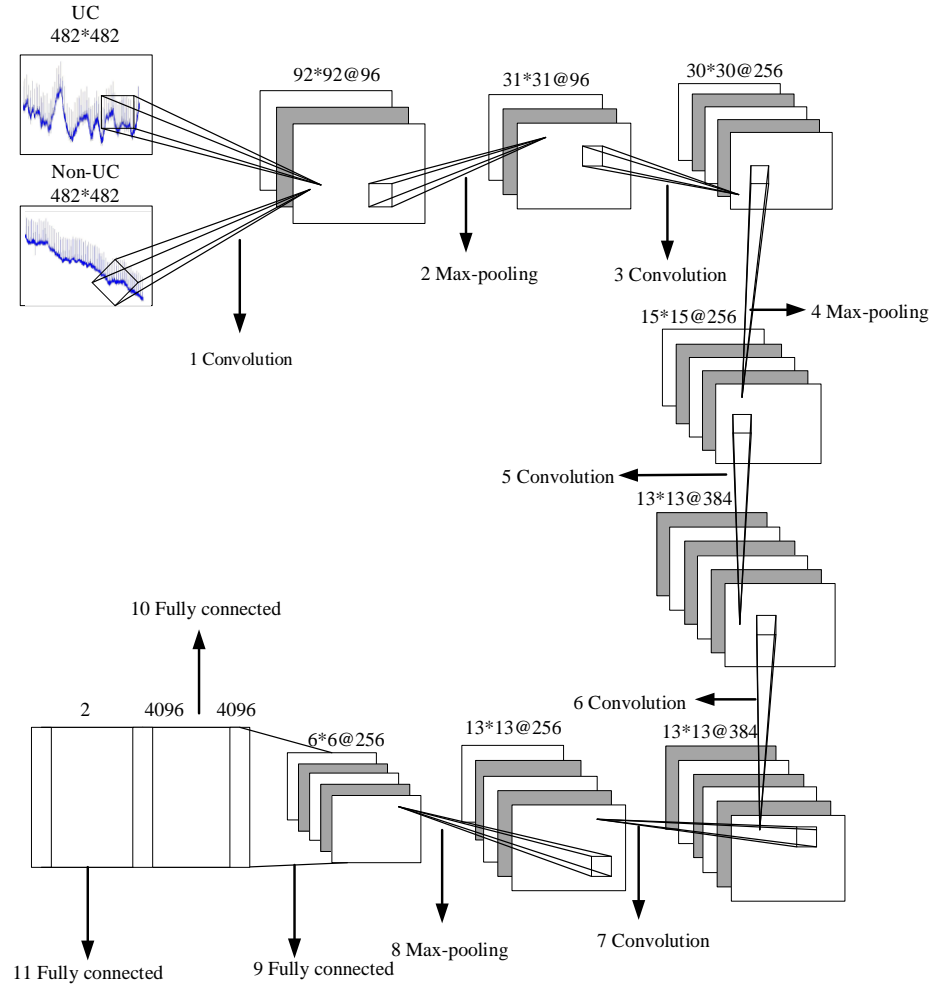


FIGURE 4 CNN architecture with eleven layers.

TABLE 1 The detailed parameters of the CNN

Layer	Type	Kernel Size	Other Parameters	output
1	Conv+ReLU	27	Stride=5	92*92@96
2	Max-pooling	2	Stride=3	31*31@96
3	Conv+LRN+ReL	2	Stride=1	30*30@256
4	Max-pooling	2	Stride=2	15*15@256
5	Conv+LRN+ReL	3	Stride=1	13*13@384
6	Conv+ReLU	3	Stride=1, pad =2	13*13@384
7	Conv+ReLU	3	Stride=1, pad =2	13*13@256
8	Max-pooling	3	Stride=2	6*6@256
9	FC+ReLU		Dropout_ratio =0.5	4096
10	FC+ReLU		Dropout_ratio =0.5	4096
11	FC+ReLU			4096

* *Pad* is the number of zero padding

CNN was running on a workstation using Linux Ubuntu 16.04 LTS Operating System, and CPUs of Intel Xeon(R) and E5-2630 v4 @2.2GHz *20.

2.2.4 EHG Classification using convolutional neural network

The CNN was established to recognize UC and non-UC segments using EHG signals collected by the 8-electrode and 4-electrode configurations separately. From each 8-electrode structure, 7,152 UC and non-UC images were obtained, of which 4,768 were used for training, 1,192 for validation, and 1,192 for testing CNN. Similarly, 3576 images were obtained from each 4-electrode configuration, 2384 images of which were used for training, 596 images for validating and 596 images for testing CNN. The classification results were evaluated by the method of five-fold-cross-validation. The hyper-parameters of CNN were optimized by using the validation data. The mean of AUC and accuracy over the test sets was calculated respectively to evaluate the classification results.

Receiver operating characteristic (ROC) curve is an authoritative method to summarize classifier performance in a series of trade-offs between true positive (TP) and false positive (FP) rates. The area under the curve (AUC) is an acceptable performance index of ROC curve. In the study, TP is the number of correctly classified UCs and FP is the number of incorrectly classified UCs.

2.2.5 Electrode configuration scoring method

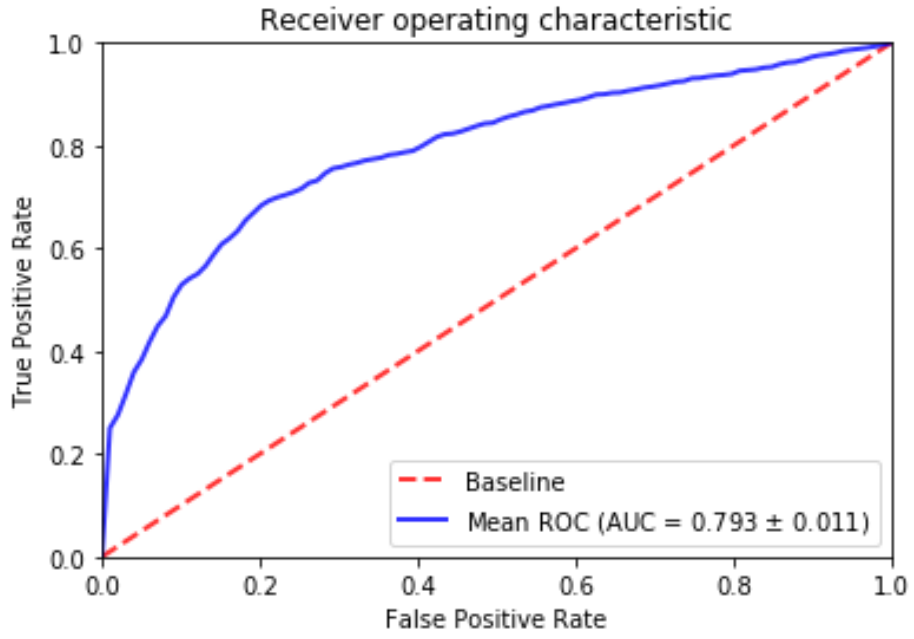
Based on the class results, each chosen electrode configuration was scored. AUC was considered to be a better measurement method based on formal definitions of discriminability and consistency. Therefore, AUC was more important than accuracy when evaluating and comparing different electrode configurations. The score of each configuration was calculated as follow:

$$\text{Score} = \text{AUC} \times \text{weight} + \text{accuracy} \quad (1)^{30-31}$$

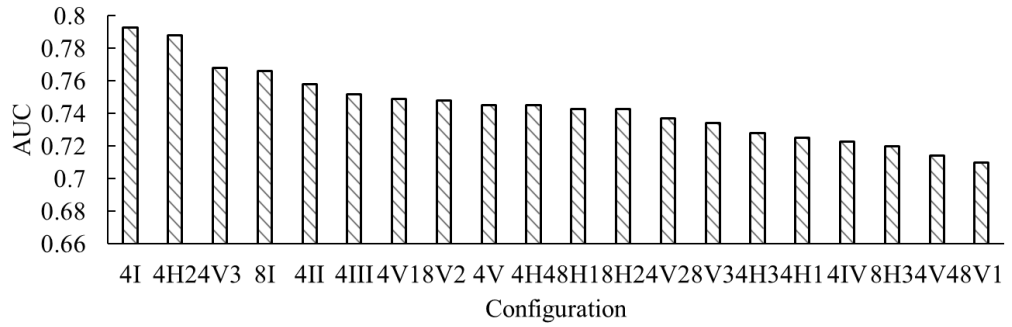
where the “weight,” a positive integer ranging from 2 to 10, is used to stress the importance of AUC.³⁰⁻³¹

3 RESULTS

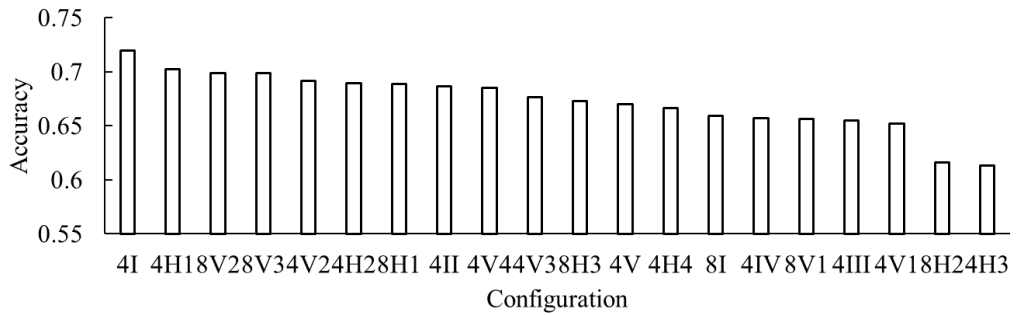
ROC curve was depicted and AUC was calculated for each 4-electrode and 8-electrode configuration. Figure 5 (A) gives an example of ROC from 4I with an AUC of 0.793 (95% confidence interval (CI) : 0.71–0.88, P= 0.0021). The AUC and accuracy of the selected 4-electrode and 8-electrode configurations are shown in Figure5 (B) and (C) respectively. For AUC, 4I> 4H2> 4V3> 8I> 4II> 4III> 4V1> 8V2> 4V= 4H4> 8H1= 8H2> 4V2> 8V3> 4H3> 4H1> 4IV> 8H3> 4V4> 8V1. For accuracy, 4I> 4H1> 8V2> 8V3> 4V2> 4H2> 8H1> 4II> 4V4> 4V3> 8H3> 4V> 4H4> 8I> 4IV> 8V1> 4III> 4V1> 8H2>4H3.



(A)



(B)



(C)

FIGURE 5 Performance of CNN with 4-electrode and 8-electrode configurations. (A) An example of a ROC curve from 8I (B) AUC of different electrode configurations (C) Accuracy of different electrode configurations

Score top 3 electrode configurations with different weights are shown in table 2. The results from the weight 1 were different from the other weights. The weight values from 2 to 10 do not influence the ranking of the top 3, and therefore, the minimum weight of 2 was chosen to calculate the score of different electrode configurations.

TABLE 2 Score top 3 electrode configuration with different weights

Rank	Weight	1	2	3	4	5	6	7	8	9	10
	R1		4I	4I	4I	4I	4I	4I	4I	4I	4I
R2		4H2	4H2	4H2	4H2	4H2	4H2	4H2	4H2	4H2	4H2

*R1: rank the first; R2: rank the second; R3: rank the third.

The score of each 4-electrode and 8-electrode configuration with the weight of 2 is shown in Figure 6. The score was ranked as: 4I> 4H2> 4V3> 4II> 8V2> 8I> 8H1> 8V3> 4V2> 4V> 4III> 4H4> 4H1> 4V1> 4V4> 8H3> 4IV> 8H2> 8V1> 4H3.

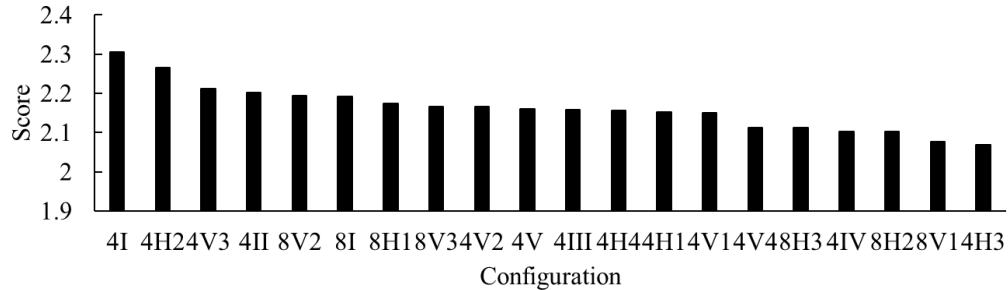


FIGURE 6 The 4-electrode and 8-electrode configurations sorted from high score to low score

4 DISCUSSION

One of the impediments of conventional TOCO was the restricted mobility of pregnant women during labor, and therefore a lighter, smaller, or wireless system was required. Many authors confirmed that EHG signals could be used as a noninvasive method to evaluate the electrical activity of uterus.^{21, 32} The Icelandic database provided EHG signals recorded with 16 electrodes. Reducing the number of electrodes that used to record EHG is essential for the convenience of pregnant women, particularly when a continuous monitoring time is demanded. Using too many electrodes on a patient could limit their movements and created stress. We expect to obtain more information with fewer electrodes. Efforts to reduce the number of electrodes have brought many benefits because some monitoring and experimental processes require patient movement.

This paper studied the effect of electrode configuration on UC recognition according to CNN performance and score ranking. CNN is a class of deep, feed-forward ANN, which has not been widely used for EHG classification as far as we know. Among the selected electrode configurations, 4I was found to be optimal for classifying UC and non-UC EHG segments. Compared with the reported methods of EHG channel combination selection,^{23, 33} our proposed method was not relying on feature extraction and selection algorithms and yet achieved acceptable results.

Among the present electrode configurations, the four electrodes with 4I configuration covering the upper right part of the uterus achieved the best results. The obstetric textbooks generally consent that UCs originate in the upper corner of the uterus and propagate downward.³⁴ However, this viewpoint has been debated recently with the work of Rabotti's team concerning the conduction velocity of the EHG's,³⁵ and by Young, concerning the mechanotransduction effect due to the presence of channels sensitive to stretching.³⁶ Diab's analysis of the evolution of the real sources during contraction showed a non linear propagation of uterine electrical activity.³⁷ Steigrad and Strecker found that about 80% of women in pregnancy have uterus torsion to the right.³⁸⁻³⁹ Therefore, it is reasonable to infer that EHG signals from 4I configuration provide more useful information for distinguishing between UCs and non-UCs. The optimal electrode configuration varies with the purpose of the application. As to the diagnosis of preterm labor with EHG recordings, the electrode configurations applied were similar to 4V and 8V2.^{10, 13} In addition to the adjacent horizontal and vertical configurations, other configurations along various directions was be helpful to understand the origin and spread of uterine contractions, and to explore the EHG methods for the diagnosis of premature delivery. Also, the ability of each electrode to recognize UC will be investigated.

The scoring method for the electrode configuration has to be investigated further. The weight value was used to regulate the importance of AUC and accuracy. AUC has been conventionally used in the medical diagnosis, which should be preferred over accuracy for evaluating the predictive ability of classifiers.³⁰ In our study, the AUC and accuracy were used alone to evaluate the electrode configuration, as shown in Fig5 (B) and (C). However, their results were different. With comprehensive consideration, AUC and accuracy were combined to evaluate electrode configuration. AUC is suitable for both the balanced or unbalanced datasets because it comprehensively considers both the TP rate and FP rate. The sensitivity of accuracy to the majority and minority class may lead to the deviation of classification. Our proposed method can be generalized to distinguish between the majority class (term delivery) and the minority class (preterm delivery) in the future.

CNN was firstly used for image evaluation so that many of its features were based on image representation, and there is a mature CNN parameter adjustment platform for image classification.²⁶ The two-dimensional (2-D) CNN is more effective in processing small datasets,⁴⁰⁻⁴¹ although one-dimensional (1-D) CNNs have recently been applied to the classification of time series (such as ECG signals).²⁸ So in the first round of testing, the time series of EHG signals were segmented and converted into images, which were applied to CNN. The performance of CNN could be further improved with the increase of EHG signals. We'll choose to work with 1D CNN and process signals as a time series in the future. Once the CNN and electrode configuration were determined, UCs could be detected in real-time for all patients. Therefore, wearable UC could be monitored in clinic for a long time, and the automatic recognition system could be used to recognize UCs.

In our study, we agreed that EHG signals still contained other interference components even after the preprocessing. The automatic identification of UCs and motion artifacts has been proposed recently,⁴² which may facilitate the CNN training. We manually determined the EHG segments corresponding to UCs based on the TOCO and comments of UCs. The EHG segments with too much interference were not used for CNN training. Automatic identification of contractions and motion artifacts will be investigated in future study. Besides, it is more appropriate to establish CNN models with different EHG signals associated with terms. However, we used the same trained CNN for all patients and electrode configurations because of the small datasets. More clinical cases of varied gestational age would be collected in follow-up research.

To sum up, this study finds a new method combining CNN classification and scoring to evaluate electrode configurations, which is used to identify UCs in EHG signals. Among the electrode configurations we have attempted, the 4-electrode configuration covering the upper left of the uterus is optimal for identifying UCs in EHG signals. The reduced number of electrodes will bring convenience for UC monitoring in practice, and has a good prospect in obstetric clinical application.

ACKNOWLEDGMENTS

This research was funded by National Key R&D Program of China (2019YFC0119700), Bill & Melinda Gates Foundation (OPP1148910), Beijing Natural Science Foundation (7172015), Beijing Science and Technology Project (Z161100000116005).

COMPLIANCE WITH ETHICAL STANDARDS

Conflict of Interest All Authors declare that they have no conflict of interest.

Statement of Original All authors have contributed to the creation of this manuscript for important intellectual content to the field uterine EMG analysis and labor prediction and read and approved the final manuscript.

Ethical Approval This article does not contain any studies with human participants or animals performed by any of the authors.

REFERENCE

1. Lammers WJEP. The electrical activities of the uterus during pregnancy. *Reprod Sci.* 2012;20:182-189. <https://doi.org/10.1177/1933719112446082>.
2. Steer P, Flint C. ABC of labour care: physiology and management of normal labour. *BMJ.* 1999;318:793-796. <https://doi.org/10.1136/bmj.318.7186.793>.
3. Garfield RE, Maner WL. Physiology and electrical activity of uterine contractions. *Semin Cell Dev Biol.* 2007;18:289-295. <https://doi.org/10.1016/j.semcdb.2007.05.004>.
4. Haran G, Elbaz M, Fejgin MD, Biron-Shental T. A comparison of surface acquired uterine electromyography and intrauterine pressure catheter to assess uterine activity. *Am J Obstet Gynecol.* 2012;206:412.e1-412.e5. <https://doi.org/10.1016/j.ajog.2011.12.015>.
5. Garcia-Casado J, Ye-Lin Y, Prats-Boluda G, Mas-Cabo J, Alberola-Rubio J, Perales A. Electrohysterography in the diagnosis of preterm birth: a review. *Physiol Meas.* 2018;39(2):02TR01. <https://doi.org/10.1088/1361-6579/aaad56>.
6. Vlemminx MWC, Rabotti C, van der Hout-van der Jagt MB, Oei SG. Clinical use of electrohysterography during term labor. *Obstet Gynecol Surv.* 2018;73(5):303–324. <https://doi.org/10.1097/ogx.0000000000000560>.
7. Alberola-Rubio J, Prats-Boluda G, Ye-Lin Y, Valero J, Perales A, Garcia-Casado J. Comparison of non-invasive electrohysterographic recording techniques for monitoring uterine dynamics. *Med Eng Phys.* 2013;35:1736-1743. <https://doi.org/10.1016/j.medengphy.2013.07.008>.
8. Hassan MM, Terrien J, Muszynski C, Alexandersson A, Marque C, Karlsson B. Better pregnancy monitoring using nonlinear correlation analysis of external uterine electromyography. *IEEE Trans Biomed Eng.* 2013;60:1160-1166. <https://doi.org/10.1109/tbme.2012.2229279>.
9. Alexandersson A, Steingrimsdottir T, Terrien J, Marque C, Karlsson B. The Icelandic 16-electrode electrohysterogram database. *Sci Data.* 2015;2:150017. <https://doi.org/10.1038/sdata.2015.17>.
10. Fele-Žorž G, Kavšek G, Novak-Antolicević Ž, Jager F. A comparison of various linear and non-linear signal processing techniques to separate uterine EMG records of term and pre-term delivery groups. *Med Biol Eng Comput.* 2008;46(9):911-922. <https://doi.org/10.1007/s11517-008-0350-y>.
11. Lucovnik M, Maner WL, Chambliss LR, et al. Noninvasive uterine electromyography for prediction of preterm delivery. *Am J Obstet Gynecol.* 2011;204:228.e1-228.e10. <https://doi.org/10.1016/j.ajog.2010.09.024>.
12. Maner WL, Garfield RE. Identification of human term and preterm labor using artificial neural networks on uterine electromyography data. *Ann Biomed Eng.* 2007;35:465-473. <https://doi.org/10.1007/s10439-006-9248-8>.
13. Lemancewicz A, Kuc P, Doroszkiewicz K, et al. Early diagnosis of threatened premature labor by electrohysterographic recordings. *Int J Gynecol Obstet.* 2012;119(S3):S398. [https://doi.org/10.1016/s0020-7292\(12\)60819-4](https://doi.org/10.1016/s0020-7292(12)60819-4).
14. McDonald SC, Brooker G, Phipps H, Hyett J. The identification and tracking of uterine contractions using template based cross-correlation. *Ann Biomed Eng.* 2017;45:2196-2210. <https://doi.org/10.1007/s10439-017-1873-x>.
15. Ye-Lin Y, Garcia-Casado J, Prats-Boluda G, Alberola-Rubio J, Perales A. Automatic identification of motion artifacts in EHG recording for robust analysis of uterine contractions. *Comput Math Methods Med.* 2014;2014:1-11. <https://doi.org/10.1155/2014/470786>.
16. De Lau H, Rabotti C, Oosterbaan HP, Mischi M, Oei GS. Study protocol: PoPE-prediction of preterm delivery by electrohysterography. *BMC Pregnancy Childbirth.* 2014;14:192. <https://doi.org/10.1186/1471-2393-14-192>.
17. Verdenik I, Pajntar M, Leskošek B. Uterine electrical activity as predictor of preterm birth in women with preterm contractions. *Eur J Obstet Gynecol Reprod Biol.* 2001;95:149-153. [https://doi.org/10.1016/s0301-2115\(00\)00418-8](https://doi.org/10.1016/s0301-2115(00)00418-8).

18. Gao P, Hao D, An Y, et al. Comparison of electrohysterogram signal measured by surface electrodes with different designs: a computational study with dipole band and abdomen models. *Sci Rep.* 2017;7:17282. <https://doi.org/10.1038/s41598-017-17109-3>.
19. Ye-Lin Y, Alberola-Rubio J, Prats-boluda G, Perales A, Desantes D, Garcia-Casado J. Feasibility and analysis of bipolar concentric recording of electrohysterogram with flexible active electrode. *Ann Biomed Eng.* 2014;43:968-976. <https://doi.org/10.1007/s10439-014-1130-5>.
20. Garcia-Casado J, Ye-Lin Y, Prats-Boluda G, Makeyev O. Evaluation of bipolar, tripolar, and quadripolar Laplacian estimates of electrocardiogram via concentric ring electrodes. *Sensors.* 2019;19(17):3780. <https://doi.org/10.3390/s19173780>.
21. Alamedine D, Diab A, Muszynski C, Karlsson B, Khalil M, Marque C. Selection algorithm for parameters to characterize uterine EHG signals for the detection of preterm labor. *Signal Image Video Process.* 2014;8:1169-1178. <https://doi.org/10.1007/s11760-014-0655-2>.
22. Alamedine D, Khalil M, Marque C. Comparison of different EHG feature selection methods for the detection of preterm labor. *Comput Math Methods Med.* 2013;2013:1-9. <https://doi.org/10.1155/2013/485684>.
23. Moslem B, Diab MO, Khalil M, Marque C. Classification of multichannel uterine EMG signals using a reduced number of channels. Paper presented at: 8th International Symposium on Mechatronics and Its Applications; 10-12 April, 2012, Sharjah, United Arab Emirates. <https://doi.org/10.1109/isma.2012.6215191>.
24. Fergus P, Idowu I, Hussain A, Dobbins C. Advanced artificial neural network classification for detecting preterm births using EHG records. *Neurocomputing.* 2016;188:42-49. <https://doi.org/10.1016/j.neucom.2015.01.107>.
25. Jarrett K, Kavukcuoglu K, Ranzato MA, LeCun Y. What is the best multi-stage architecture for object recognition? Paper presented at: IEEE 12th International Conference on Computer Vision; 29 Sept.-2 Oct. 2009. Kyoto, Japan. <https://doi.org/10.1109/iccv.2009.5459469>.
26. Krizhevsky A, Sutskever I, Hinton GE. ImageNet classification with deep convolutional neural networks. *Commun ACM.* 2017;60:84-90. <https://doi.org/10.1145/3065386>.
27. Acharya UR, Fujita H, Oh SL, et al. Automated identification of shockable and non-shockable life-threatening ventricular arrhythmias using convolutional neural network. *Future Gener Comput Syst.* 2018;79:952-959. <https://doi.org/10.1016/j.future.2017.08.039>.
28. Kiranyaz S, Ince T, Gabbouj M. Real-time patient-specific ECG classification by 1-D convolutional neural networks. *IEEE Trans Biomed Eng.* 2016;63:664-675. <https://doi.org/10.1109/tbme.2015.2468589>.
29. Devedeux D, Marque C, Mansour S, Germain G, Duchêne J. Uterine electromyography: a critical review. *Am J Obstet Gynecol.* 1993;169:1636-1653. [https://doi.org/10.1016/0002-9378\(93\)90456-s](https://doi.org/10.1016/0002-9378(93)90456-s).
30. Huang J, Ling CX. Using AUC and accuracy in evaluating learning algorithms. *IEEE Trans Knowl Data Eng.* 2005;17:299-310. <https://doi.org/10.1109/tkde.2005.50>.
31. Ling CX, Huang J, Zhang H. AUC: a better measure than accuracy in comparing learning algorithms. *Lect Notes Comput Sci.* 2003;2671:329-341. https://doi.org/10.1007/3-540-44886-1_25.
32. Alamedine D, Khalil M, Marque C. Parameters extraction and monitoring in uterine EMG signals. Detection of preterm deliveries. *IRBM.* 2013;34:322-325. <https://doi.org/10.1016/j.irbm.2013.08.003>.
33. Alamedine D, Khalil M, Marque C. Channel combination selection for EHG bivariate analysis. Paper presented at: 3rd Middle East Conference on Biomedical Engineering (MECBME); 6-7 Oct. 2016, Beirut, Lebanon. <https://doi.org/10.1109/mecbme.2016.7745408>.
34. Coad J, Dunstall M, eds. *Anatomy and Physiology for Midwives.* London, UK: Churchill Livingstone; 2001.

35. Rabotti C, Mischi M. Propagation of electrical activity in uterine muscle during pregnancy: a review. *Acta Physiol.* 2014;213:406-416. <https://doi.org/10.1111/apha.12424>.
36. YOUNG RC. Myocytes, myometrium, and uterine contractions. *Ann NY Acad Sci.* 2007;1101(1):72–84. <https://doi.org/10.1196/annals.1389.038>.
37. Steigrad SJ. Torsion of the gravid uterus. *Aust NZ J Obstet Gynaecol.* 1987;27:66-68. <https://doi.org/10.1111/j.1479-828x.1987.tb00939.x>.
38. Zahran S, Diab A, Khalil M, Marque C. Source localization of uterine activity using maximum entropy on the mean approach. Paper presented at: IEEE Middle East Conference on Biomedical Engineering; IEEE; 28-30 March 2018:247-251; Tunis, Tunisia.
39. Strecker W, Keppler P, Gebhard F, Kinzl L. Length and torsion of the lower limb. *J Bone Joint Surg.* 1997;79-B:1019-1023. <https://doi.org/10.1302/0301-620x.79b6.0791019>.
40. Wu Y, Yang F, Liu Y, et al. A Comparison of 1-D and 2-D Deep Convolutional Neural Networks in ECG Classification[J]. Conference proceedings: Annual International Conference of the IEEE Engineering in Medicine and Biology Society. IEEE Engineering in Medicine and Biology Society. Conference. 1 July 2018; Hawaii, USA. 2018:324-327.
41. Zha X. A comparison of 1-D and 2-D deep convolutional neural networks in ECG classification; 2018.
42. Kim M-G, Ko H, Pan SB. A study on user recognition using 2D ECG based on ensemble of deep convolutional neural networks. *J Amb Intel Human Comput.* 2019;11:1859-1867. <https://doi.org/10.1007/s12652-019-01195-4>.
43. Zaylaa A, Diab A, Khalil M, Marque C. Multichannel EHG segmentation for automatically identifying contractions and motion artifacts. Paper presented at: Fourth International Conference on Advances in Biomedical Engineering (ICABME); 2017. Beirut, Lebanon. <https://doi.org/10.1109/icabme.2017.8167563>.